

## Electronic Supplementary Information

### **Sputtering gold nanoparticles on nanoporous bismuth vanadate for sensitive and selective photoelectrochemical aptasensing of thrombin†**

Yanmei Xin, Yina Zhao, Beilei Qiu, and Zhonghai Zhang\*

*School of Chemistry and Molecular Engineering, East China Normal University, Dongchuan Road 500, Shanghai 200241, China*

*Address correspondence to [zhzhang@chem.ecnu.edu.cn](mailto:zhzhang@chem.ecnu.edu.cn)*

#### **Experimental Section**

**Chemicals and Materials.** Fluorine doped tin oxide (FTO) glass were purchased from Zhuhai Kaivo Optoelectronic Technology Co., Ltd. Potassium iodide (KI), nitric acid (HNO<sub>3</sub>), bismuth nitrate pentahydrate (Bi(NO<sub>3</sub>)<sub>3</sub>·5H<sub>2</sub>O), p-benzoquinone, vanadyl acetylacetonate (VO(acac)<sub>2</sub>), dimethyl sulfoxide (DMSO), ethanol, acetone, mercaptohexanol (MCH), thrombin (Tob), bovine serum albumin (BSA), streptavidin (SA), adenosine 5'-triphosphate disodium salt (ATP), and trypsin from bovine pancreas (Tps) were all purchased from Macklin Inc., Shanghai, China. The thrombin aptamer (5'-SH-(CH<sub>2</sub>)<sub>6</sub>-GGT TGGTGT GGT TGG-3') with -SH modification was purchased from Sangon Biotech (shanghai) Co., Ltd. The healthy adult blood serum was supplied from Shanghai Chaoyan Biotechnology Co., LTD. All aqueous solutions were used as received and prepared using deionized water (DI) with a resistivity of 18.2 MΩ cm.

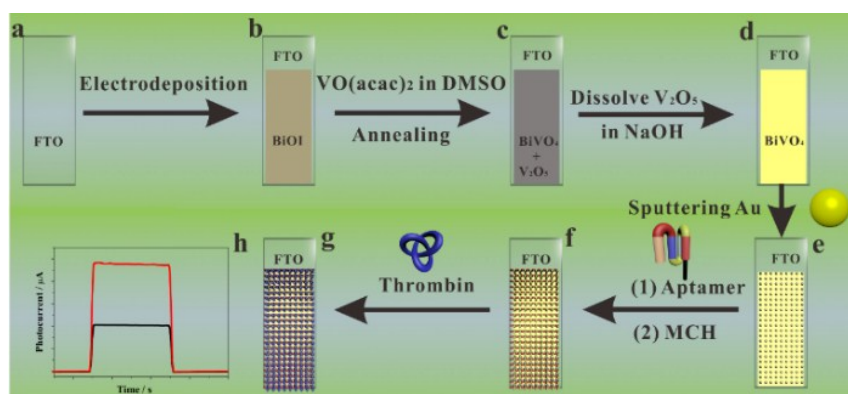
**Synthesis of BiVO<sub>4</sub> electrodes.** The BiVO<sub>4</sub> photoelectrode was synthesized as previously reported method.<sup>1</sup> The BiOI film was first electrodeposited on FTO glass with potential of -0.1 V vs Ag/AgCl in an electrolyte composed with 0.04 M Bi(NO<sub>3</sub>)<sub>3</sub>, 0.4 M KI, and 0.23 M p-benzoquinone solutions at room temperature for 5min. Then, the obtained BiOI/FTO electrode was rinsed with 0.2 mL of DMSO containing 0.2 M VO(acac)<sub>2</sub>, and followed annealing in a muffle furnace at 450 °C for 2 h. After cooling to room temperature, the electrodes were soaked in 1 M NaOH solution for 30 min with gentle stirring to remove the excess V<sub>2</sub>O<sub>5</sub> on the BiVO<sub>4</sub>. Finally, the pure BiVO<sub>4</sub> electrode was rinsed with deionized water and dried in ambient air.

**Fabrication of sAu/BiVO<sub>4</sub> PECAS.** The Au NPs were sputtered onto BiVO<sub>4</sub> by an ion sputtering instrument (JS-1600, Beijing Saintins Technology Co., Ltd.) with vacuum degree of 0.1 mbar and sputtering current of 6 mA. The deposited Au amount can be adjusted through tuning the sputtering time. The Au NPs were also deposited on BiVO<sub>4</sub> with different methods of photocatalytic reduction (*p*Au/BiVO<sub>4</sub>) and electrochemical deposition (*e*Au/BiVO<sub>4</sub>) as previously reported procedures.<sup>34,35</sup> The thrombin aptamer of 5'-SH-(CH<sub>2</sub>)<sub>6</sub>-GGT TGGTGT GGT TGG-3' was first heating to 80 °C for 5 min to ascertain its appropriate secondary structure. Then, the *s*Au/BiVO<sub>4</sub> was incubated with the aptamer in 0.1 M phosphate buffer saline (pH = 7.4) with optimized aptamer concentration for 12 h. Finally, the aptamer/*s*Au/BiVO<sub>4</sub> electrode was soaked in 1 mM MCH solution for 1 h to cover the rest exposing surface of Au NPs.

**Materials Characterization.** The morphologies of *s*Au/BiVO<sub>4</sub> were determined by scanning electron microscopy (SEM, Hitachi S4800) and transmission electron

microscopy (TEM, JEOL JEM 2100). The crystalline structure of the samples was analyzed by X-ray diffraction (XRD, Bruker D8 Discover diffractometer, using Cu K $\alpha$  radiation,  $\lambda = 1.540598 \text{ \AA}$ ). The Raman spectra were measured through DXR Raman Microscope (Thermo) with excitation of 532 nm laser. The diffuse reflectance UV-vis adsorption spectra were recorded on a spectrophotometer (Shimadazu, UV 3600) with fine BaSO<sub>4</sub> powder as reference. Photoelectron Spectroscopy (XPS) data were collected by an Axis Ultra instrument (Kratos Analytical) under ultrahigh vacuum ( $<10^{-8}$  torr) and using a monochromatic Al K $\alpha$  X-ray source operating at 150 W. Binding energies were referenced to the C 1s binding energy of 285.0 eV.

**Performance of PECAS.** The PEC performance of the PECAS were evaluated using a three-electrode system with the aptamer/sAu/BiVO<sub>4</sub>/FTO, Ag/AgCl and Pt foil as working, reference, and counter electrodes, respectively, in a supporting electrolyte of PBS (1 $\times$ , pH = 7.4) solution. The PECAS was incubated with different concentrations of thrombin at 37 °C for 20 min in PBS solution. The transient photocurrents were evaluated under chopped light irradiation from a solar simulation system (PLS-SXE300, PE300BF) with 420 nm cutoff filter at a fixed electrode potential of 0 V *vs* Ag/AgCl. The electrochemical impedance spectra (EIS) were measured using a PGSTAT 302N Autolab Potentiostat/Galvanostat (Metrohm) equipped with a frequency analyzer module (FRA2) with an excitation signal of 10 mV amplitude covering the frequency of 10<sup>5</sup>–0.1 Hz interval, and the impedance *vs* potential measurement at fixed frequency of 5 kHz was also performed to determine the carrier density through the Mott-Schottky plots.



**Scheme S1.** Schematic illustration of the PECAS. (a) FTO, (b) Electrodeposited BiOI on FTO, (c)  $\text{BiVO}_4$  and excess  $\text{V}_2\text{O}_5$ , (d)  $\text{BiVO}_4$ , (e)  $\text{sAu/BiVO}_4$ , (f) aptamer/ $\text{sAu/BiVO}_4$ , (g) thrombin/aptamer/ $\text{sAu/BiVO}_4$ , and (h) potential photocurrent response.

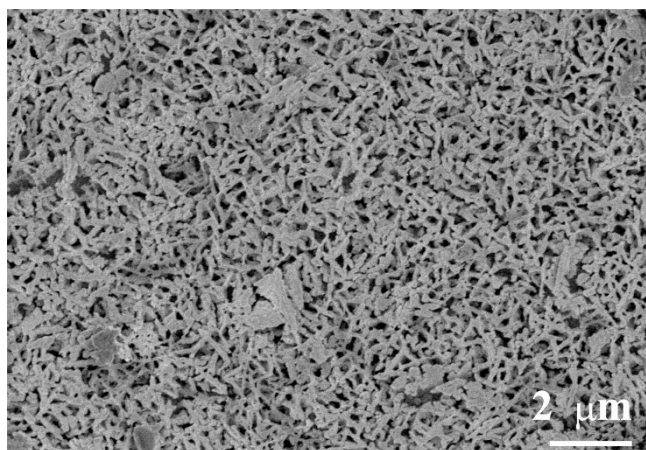


**Fig. S1** SEM image of BiOI.

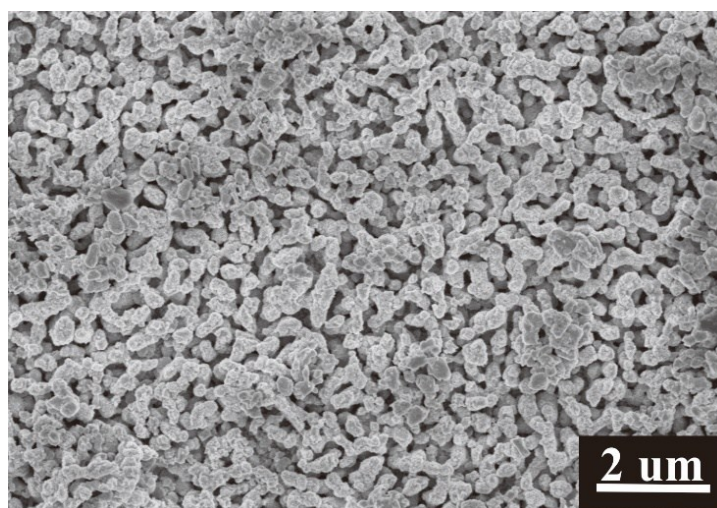


**Fig. S2** Scanning electron microscopic image of  $\text{BiVO}_4$ .

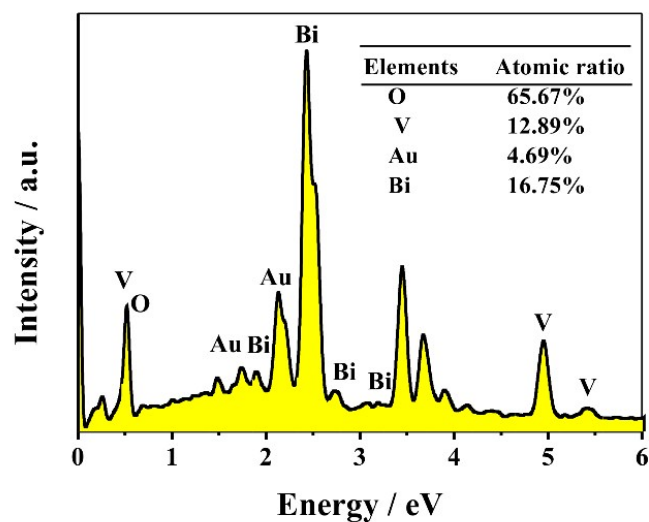


Fig. S3 Energy dispersive X-ray spectrum of *s*Au/BiVO<sub>4</sub>.

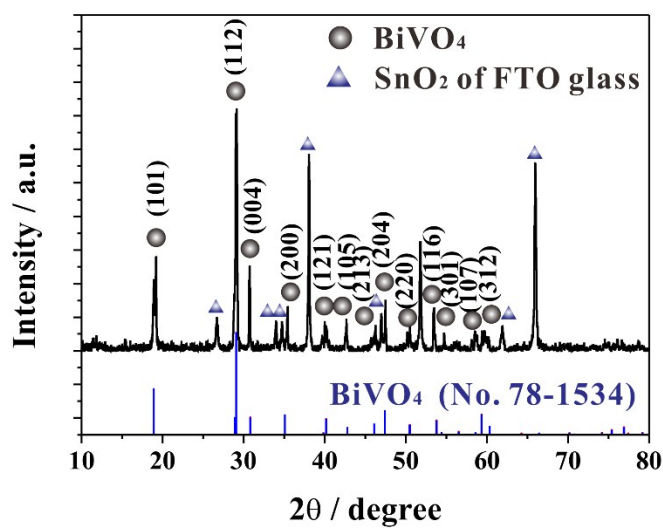
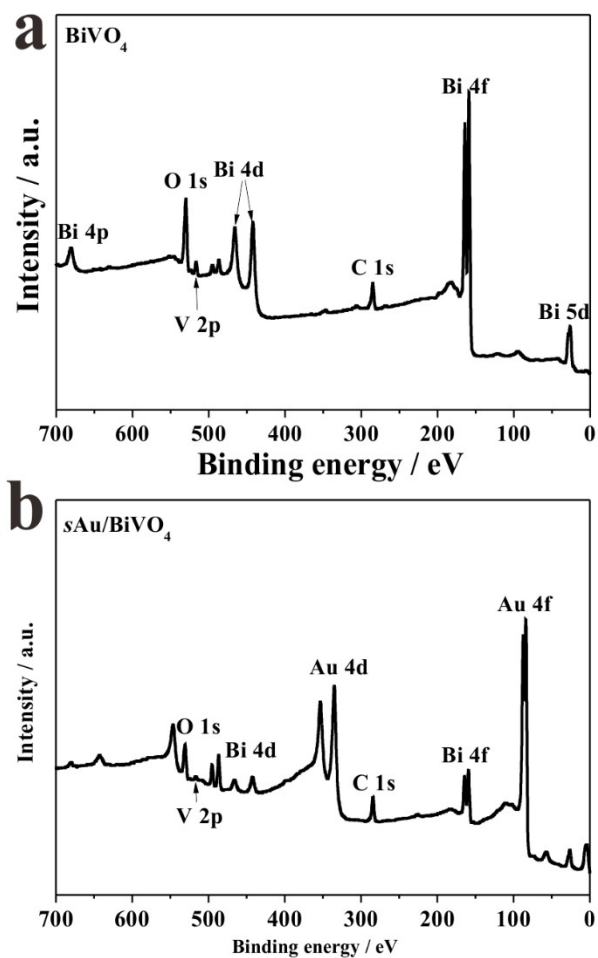
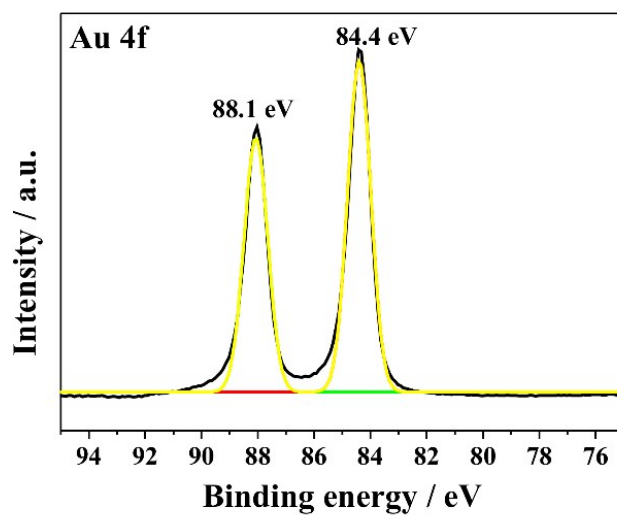


Fig. S4 XRD patterns of BiVO<sub>4</sub>.



**Fig. S5** XPS survey spectra of (a)  $\text{BiVO}_4$  and (b)  $s\text{Au}/\text{BiVO}_4$ .



**Fig. S6** Core-level XPS of Au 4f of  $s\text{Au}/\text{BiVO}_4$ .

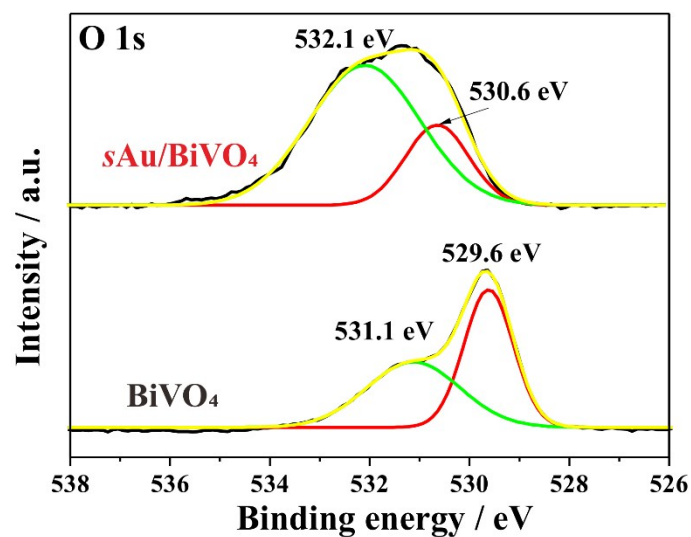


Fig. S7 Core-level XPS of O 1s of BiVO<sub>4</sub> and sAu/BiVO<sub>4</sub>.

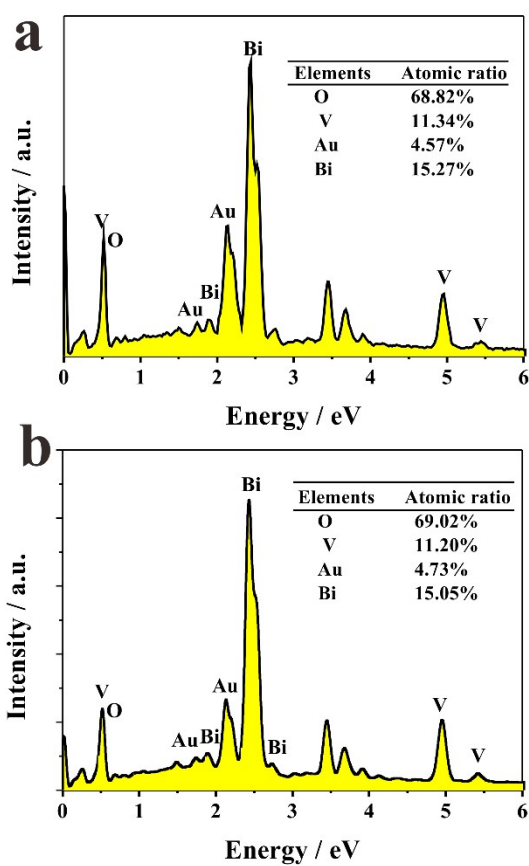
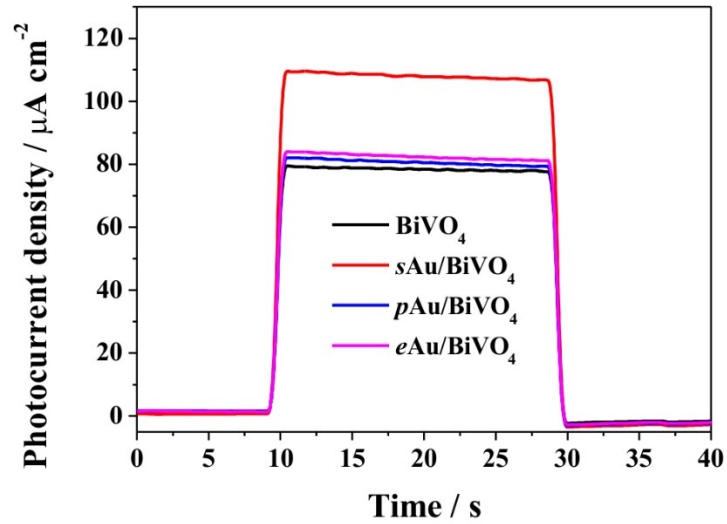
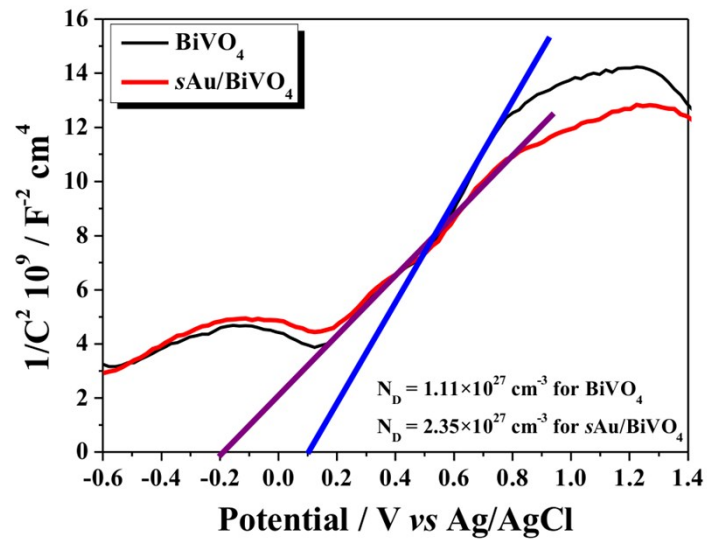


Fig. S8 EDS spectra of (a) pAu/BiOV<sub>4</sub> and (b) eAu/BiVO<sub>4</sub>.



**Fig. S9** PEC response of  $\text{BiVO}_4$  and  $s\text{Au/BiVO}_4$ ,  $p\text{Au/BiVO}_4$ , and  $e\text{Au/BiVO}_4$ .



**Fig. S10** Mott-Schottky plots collected at a frequency of 5 kHz in the dark for  $\text{BiVO}_4$  and  $s\text{Au/BiVO}_4$ .



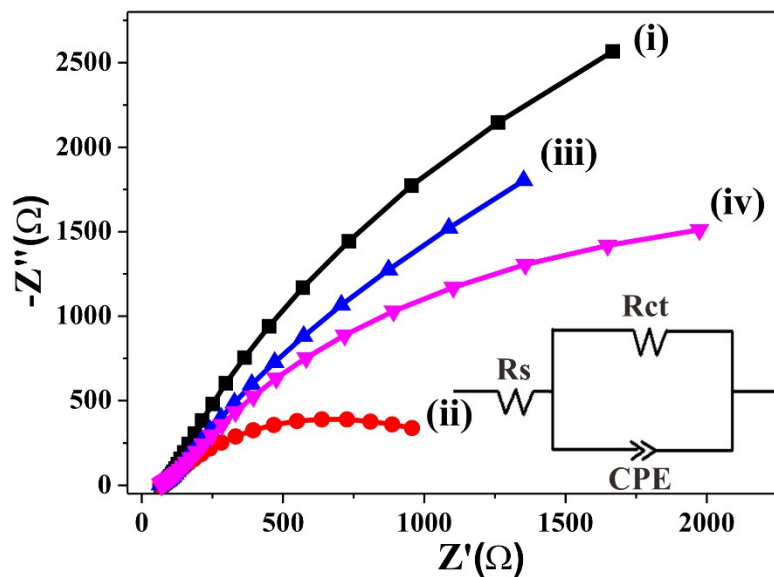


**Fig. S11** Electrochemical impedance spectra of Nyquist plots under visible light illumination of (i)  $\text{BiVO}_4$ , (ii)  $s\text{Au}/\text{BiVO}_4$ , (iii) aptamer/ $s\text{Au}/\text{BiVO}_4$ , and (iv) thrombin/aptamer/ $s\text{Au}/\text{BiVO}_4$ .

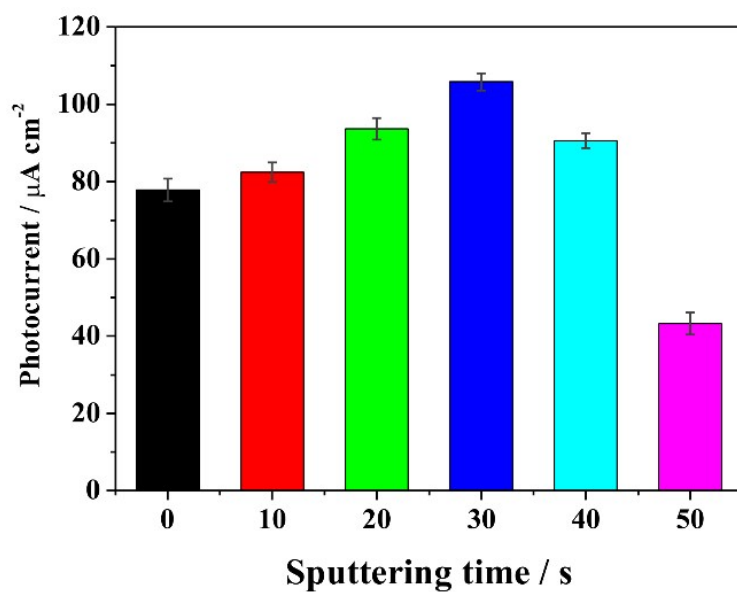


**Fig. S12** Effect of ion sputtering time on photocurrent density of  $s\text{Au}/\text{BiVO}_4$ .

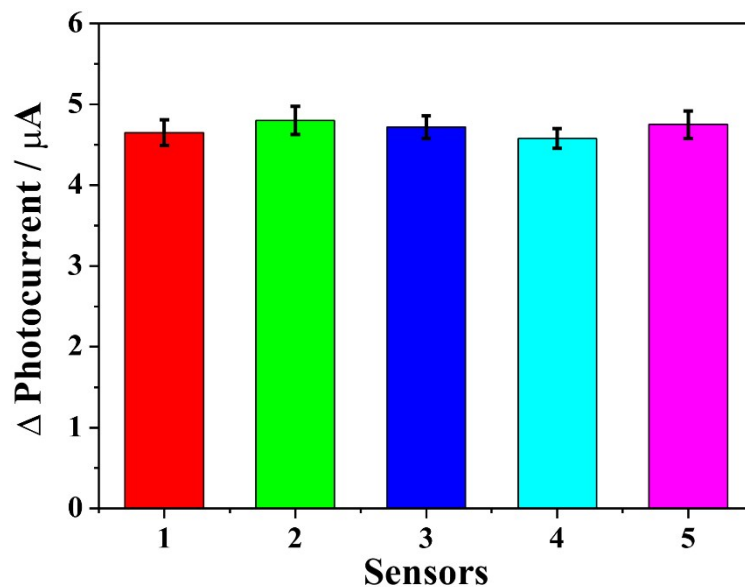


**Fig. S13** Reproducibility of five sAu/BiVO<sub>4</sub> based PECAS for detection of 100 pM thrombin.

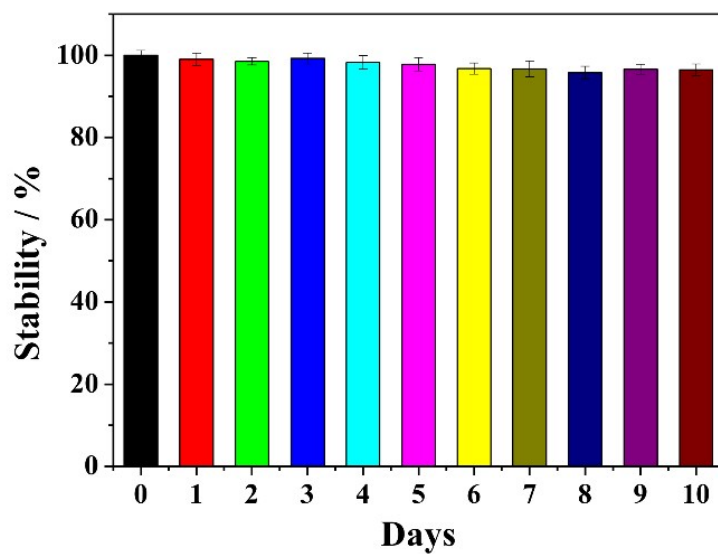


**Fig. S14** Stability of sAu/BiVO<sub>4</sub> for measurements of thrombin.

**Table S1. Comparison of various thrombin sensors**

Method	Material	Detection limit /nM	Linear range / nM	Reference
Electrochemistry	Au disk electrodes	6.4	20-768	2
Spectrophotometry	Au NPs	2	2-167	3
Surface enhanced resonance Raman scattering	Au NPs	0.1	0.1-1000	4
Chromatography	Polymer	0.1	1-500	5
Chromatography	Organic–Inorganic Hybrid Silica	67	-	6
Fluorescence	-	-	0-120	7
Electrochemistry	Graphene/Au NPs	$5.2 \times 10^{-9}$	$1.6 \times 10^{-8}$ - $5.2 \times 10^{-7}$	8
Dual polarization interferometry	-	0.5	2.5-100	9
DPV	graphene oxide	0.07	0.1-10	10
Electrochemistry	Pt/rGO	$1.5 \times 10^{-5}$	$5 \times 10^{-5}$ -60	11
PEC	CdS/graphene	$1 \times 10^{-3}$	$2 \times 10^{-3}$ -0.6	12
PEC	PbS	$1.5 \times 10^{-5}$	$10^{-4}$ -10	13
PEC	sAu/BiVO <sub>4</sub>	$0.5 \times 10^{-3}$	$10^{-3}$ -100	This work

**Table S2 The recovery of thrombin from human serum samples**

Samples	Added Tob / pM	Determined Tob / pM	RDS / %	Recovery / %
1	50	49.2	1.65	98.4
2	100	102.0	1.53	102.0
3	150	149.3	0.85	99.53
4	200	201.6	0.59	100.8

## References

- (1) T. W. Kim, K. S. Choi, *Science* **2014**, *343*, 990.
- (2) Y. Xiao, A. A. Lubin, A. J. Heeger, K. W. Plaxco, *Angew. Chem.* **2005**, *117*, 5592.
- (3) V. Pavlov, Y. Xiao, B. Shlyahovsky, I. Willner, *J. Am. Chem. Soc.* **2004**, *126*, 11768.
- (4) H. Cho, B. R. Baker, S. Wachsmann-Hogiu, C. V. Pagba, T. A. Laurence, *Nano Lett.* **2008**, *12*, 4386.
- (5) Q. Zhao, X. Li, Y. Shao, X. Le, *Anal. Chem.* **2008**, *80*, 7586.
- (6) N. Deng, Z. Liang, Y. Liang, Z. Sui, L. Zhang, Q. Wu, K. Yang, L. Zhang, Y. Zhang, *Anal. Chem.* **2012**, *84*, 10186.
- (7) A. Bini, M. Minunni, S. Centi, M. Mascini, *Anal. Chem.* **2007**, *79*, 3016.
- (8) Q. Xue, Z. Liu, Y. Guo, S. Guo, *Biosens. Bioelectronics.* **2015**, *68*, 429.
- (9) Y. Zhang, T. Hu, C. Chen, F. Yang, X. Yang, *Chem. Commun.* **2015**, *51*, 5645.
- (10) F. Ahour, M. K. Ahsani, *Biosens. Bioelectronics.* **2016**, *86*, 764.
- (11) Y. Wu, L. Zou, S. Lei, Q. Yu, B. Ye, *Biosens. Bioelectronics.* **2017**, *97*, 317.
- (12) L. Shanguan, W. Zhu, Y. Xue, S. Liu, *Biosens. Bioelectronics.* **2015**, *64*, 611.
- (13) G. L. Wang, J. X. Shu, Y. M. Dong, X. M. Wu, W. W. Zhao, J. J. Xu, H. Y. Chen, *Anal. Chem.* **2015**, *87*, 2892.